Nigerian Research Journal of Chemical Sciences (ISSN: 2682-6054)
Volume 13, Issue 2, 2025

Adsorptive Removal of Lead(II) ions from Aqueous Solutions Using Functionalized MOF-5 with Pyridine-2,6-dicarboxylic Acid

*Ogundele Damilola Tope, Adeyemi Deborah Adefunke, Olayemi Victoria Tosin,
Samsudeen Olanrewaju Azeez, Lukman Bola Abdul'rauf
Department of Chemistry and Industrial Chemistry,
Kwara State University, Malete, Nigeria
*Corresponding Author: damilola.ogundele@kwasu.edu.ng

Accepted: August 18, 2025; Published Online: August 22, 2025

ABSTRACT

Sulfonic acid, cyano and amine-functionalized MOF-5+ pyridine-2,6-dicarboxylic acid **(**PDC) were synthesized by Solvothermal method and characterized by X-ray Diffraction (XRD), Fourier Transform Infrared (FT-IR), and Scanning Electron Microscope (SEM) mapping analysis to confirm the synthesis of Metal-organic frameworks (MOFs) structures. The results of N_2 adsorption/desorption isotherm data showed that the Brunauer-Emmett-Teller (BET) surface area of the synthesized MOF-5+PDC sample was 85.98 m^2/g. The adsorption behaviour for Pb(II) ions revealed an excellent adsorption capacity of 42.5 – 57.25 mg/g, whereas the removal efficiency was over 80 - 90.9% when the initial concentration of Pb(II) ions was as low as 0.066 ppm. Design of Experimental was carried-out using Box-Behnken Design (BBD) based Response Surface Methodology (RSM) to optimize the adsorption reaction conditions at 10 – 100 mg/L for concentration, 4 – 10 for pH, and dosage of 0.01 – 0.05 g, in seventeen experimental procedures to achieve maximum adsorbed yield of Pb(II) ions. The results were within the range of 77.02 – 99.64 mg/g. The quadratic model was found to adequately predict the test amount adsorbed with an R^2 value of 0.9054. In addition, thermodynamic analysis revealed that Pb(II) adsorption is a spontaneous endothermic process. Based on the data from the study, these amine-functionalized MOFs are a promising adsorbent for the removal of Pb(II) ions from contaminated water.

Keywords: Aqueous solution, MOFs, Removal efficiency, Lead(II) ions, Adsorption, Box-Behnken Design

INTRODUCTION

The contamination of the environment with heavy metals poses a significant threat to soil and water body [1]. As awareness grows about the need to protect the environment, the removal of toxic metal ions from wastewater has become a pressing concern. Lead (Pb), a highly toxic heavy metal, has garnered considerable attention due to its environmental and toxicological implications [2,3]. Lead ions primarily enter the water environment through industrial effluents from lead smelting, battery manufacturing, printing, and mining operations [4]. Exposure to excessive levels of lead ions can cause severe damage to the kidneys, nervous system, reproductive system, and brain function [5].

The selective removal of Pb(II) ions from wastewater is crucial for environmental protection, human health, and the development of a circular economy. Various techniques, including adsorption, ion exchange, and membrane systems, have been developed to address this issue [6]. However, these methods have limitations, such as slow kinetics, low removal capacity, and poor stability and reusability. To overcome these challenges, material scientists and chemists are seeking innovative solutions that offer high capacity, selectivity, efficiency, stability, and reusability [7].

Among the available methods, adsorption stands out as a highly effective approach for extracting heavy metal ions from aqueous media, due to its affordability, simplicity, and high selectivity [5,7,8]. Metal-organic frameworks represent a novel class of porous materials that have garnered significant attention for their potential applications in various fields, including gas storage, separation, catalysis, and sensing [9].

The escalating global industrial activities have resulted in the continuous release of harmful compounds and metal ions into the water environment, posing significant environmental and health risks [10]. In this context, MOFs have emerged as promising materials for the selective removal of hazardous substances from wastewater, owing to their unique properties and potential for adsorptive applications [11]. Recently, terephthalate MOF-type materials have gained significant attention for their potential in removing various hazardous substances, including pharmaceuticals, organic dyes, alcohols, and aromatic compounds, from the environment. Metal-organic frameworks have demonstrated remarkable efficiency as water-

applicable adsorbents, playing a vital role in environmental remediation [12]. Amine-functionalized terephthalate metal-organic frameworks have garnered significant interest for mitigating the environmental hazards of lead, owing to their high surface area, extensive pore volume, and tunable pore size [12,13]. Furthermore, MOFs possess modifiable chelating sites, created by their p-columnar structures, which enable the selective recognition and adsorption of various guest molecules [14]. Certain terephthalic MOFs, such as MOF-5, have been identified as novel adsorbents, offering large pores, high surface areas, and enhanced chemical stability [15-17]. These MOFs have been successfully applied in the adsorption of pharmaceuticals, organic dyes, and aromatic compounds. Inspired by the fact that the adsorption capacity of Pb(II) ions of silica-based mesoporous materials modified by amino groups is apparently higher than that of normal silica-based materials, terephthalate MOFs with high stability after being functionalized by amino groups can probably provide many adsorptive sites to interact strongly with Pb(II) ions [18-20].

Therefore, this study aims to investigate the adsorptive removal of lead from aqueous solutions using amine, cyano and sulfonic acid functionalized terephthalic acid (1,4-benzenedicarboxylic acid and 2,6-pyridinedicarboxylic acid) as an organic linker in MOFs structure network, which was connected by three-dimensional (3D) lattices functionalized by amine compound to enhance the adsorption capacity toward noxious lead(II) metals from solution.

This research presents a highly effective adsorbent for the removal of lead(II) ions from contaminated water, demonstrating its capability to remove high concentrations of lead. The adsorbent material was characterized using FT-IR, SEM-EDX, XRD, and BET techniques. The study also investigated the effects of various parameters, including solution pH, initial lead ion concentrations, contact time, and competitive ions. The modification of amino groups on the pore surface of terephthalate metal-organic frameworks provided chelating binding sites for Pb(II) ion adsorption, which coordinated effectively with the nitrogen atoms of the amino groups [21]. The research examines the adsorption capacity, kinetics, selectivity, and applicability of the adsorbent for removing lead (II) ions from environmental water samples.

MATERIALS AND METHODS

Materials and Reagents

All chemicals were of analytical grade, purchased from commercial sources and used without further purification. *Ligands*: Terephthalic acid (TPA) and 2,6-Pyridinedicarboxylic acid. *Functionalizing Agent*: Metal Salts**:** Zn $(NO_3)_2.6H_2O$, *Solvents*: N,N'-dimethylformamide, and Deionized water.

Synthesis of MOFs

Synthesis of MOF-5+PDC

The method used for synthesis of MOF-5+PDC was solvothermal based on the report of Li et al [22], with a slight modification and adoption of the synthesis of UIO-66. 0.54 g of $Zn(NO_3)_2.6H_2O$ (2 mmol), 0.167 g of 2,6-pyridinedicarboxylic acid (1mmol) and 0.33 g of 1,4 -benzenedicarboxylic acid (2 mmol) were dissolved in 20 mL of N,N –dimethylformamide (DMF). The reaction mixtures were sealed in an autoclave and refluxed at 120^oC for 24 h. The resulting solid was filtered and washed repeatedly with DMF and dried at room temperature.

Amine- functionalization

Amine functionalization of the MOFs was conducted based on the procedure described by Luo et al [23], in which 0.1 g of the synthesized NH_2MOF-5+PDC material was suspended in 10 ml anhydrous toluene. Then, 1 ml of ethylenediamine was added to the suspension and the mixture was stirred at room temperature for 24 hours. The resulting solid was filtered and dried at 100^oC for three hours.

Sulphonic acid functionalization

The MOF-5+PDC (0.1 g) was suspended in 10 mL anhydrous toluene. Amino-methanesulfonic acid (0.11 g of 1 mmol) in toluene 5 ml was added and the mixture was stirred at room temperature for 24 hours. The resulting solid was filtered and dried at 100^oC for three hours

Cyano-functionalization

MOF-5+PDC sample of about 0.1g was suspended in 10 ml anhydrous toluene in a conical flask. Malononoitrile (0.132 g of (2 mmol)) was added to the suspension and the mixture was stirred at

room temperature for 24 hours. The resulting solid was filtered and dried at 100°C for three hours

Characterization

Powder X-ray diffraction patterns of the samples were obtained using Rigaku D/MaxIIIC, PW1800. Fourier transform infrared spectra were recorded on a SHIMAZU-FTIR (FTIR-8400s) apparatus via KBr method. The morphologies and the microstructure of the synthesized samples were characterized by scanning electron microscopy operated on a JEOL-JSM-7600F. The BET surface area measurement was performed with N_2 adsorption−desorption isotherms at liquid nitrogen temperature (77 K) after the samples were dehydrated under vacuum at 383 K for 12 h using a Micromeritics TriStar II 3020. A ContrAA 700 (Analytik Jena, Germany) high resolution continuum source atomic absorption spectrometer (AAS) was used for the determination of Pb (II) ions.

TGA Analysis

TGA 4000 PerkinElmer was used for this analysis. A small quantity of MOF 53 was put into the sample holder, placed in the analysis chamber, covered on the cheallar and allowed to cool to 15 degree Celsius. Then, the desktop computer connected to the equipment was double-clicked on the equipment shortcuts, and allowed to be operated. All the information about the sample were put in, and the nitrogen flow was opened at rate of 20 times. Finally the *start* was clicked to start the analysis.

Adsorption Studies for Pb(II) Ions

Batch Adsorption Experiments

All adsorption experiments were conducted in batches following a procedure reported by Guo et al [24]. Adsorption of Pb(II) ions metals unto the functionalized MOFs was investigated using spiked samples containing various metal concentrations (10 – 100 mg/l). Solution of the spiked samples (50 mL) was agitated with 0.1 g of MOF adsorbents at 150 rpm for 240 min at 298 K while the pH is adjusted to 6. The sample solution was separated from the MOF adsorbents via centrifugation and the residual metal concentration was determined using AAS. The effects of

operational parameters such as pH, contact time and adsorbent dosage were optimized using the Design expert software. The quantity of metal ion absorbed will be estimated using the formula in Equation 1:

$$q = \left(\frac{Ci-Cf}{m}\right) v \quad (1)$$

Where q is the adsorption capacity of a (mg/g), Ci and Cf are the initial and final concentrations of the adsorbate respectively, v is the volume of solution used (mL) and m is the mass (g) of the adsorbents.

Adsorption Thermodynamic Experiments

Thermodynamic study shows the effect of temperature on the adsorption process of functionalized MOFs. Generally, there are two common types: endothermal and exothermal sorption processes. If the sorption increases with increasing temperature, it means that the sorption is an endothermal process. Whereas the adsorption decreases with increasing temperature, indicates the exothermal adsorption process.

The thermodynamic parameters such as free energy (ΔG_0), enthalpy (ΔH_0) and entropy changes (ΔS_0) for the sorption are calculated using the following equations:

$$\Delta G = -RT\, InK \quad (2)$$

$$InK = \frac{\Delta S}{R} - \frac{\Delta H}{T} \quad (3)$$

$$\Delta G = \Delta H - T\Delta S \quad (4)$$

Where R is the ideal gas constant (kJ mol^{-1} K^{-1}), K=Cads/Ceq and T is the temperature (K). ΔH^o and ΔS^o value can be obtained from the slope and intercept respectively of Van't Hof plots of In K versus 1/T [25].

Optimization

The following parameters were optimized using Design expert software: (1). Concentration, (2). Adsorbent dosage, (3). pH and (4). Contact time at various design conditions

RESULT AND DISCUSSIONS

FT-IR Analysis of MOF-5+PDC

The FT-IR spectrum of MOF-5+PDC displayed characteristic bands at 3490 cm^{-1} corresponded to O-H stretching as presented in Figure 1**.** Two absorption bands at 3120 and 2978 cm^{-1} were assigned to C-H stretching vibrations of the methylene group. The vibration bands appearing at 1700–1500 cm^{-1} which were assigned to the carboxylic functionality of the 1,4-benzenedicarboxylate. The strong peak appeared at 1790 cm^{-1} can be attributed to C=O stretching vibration of the carboxylate group of MOF-5@PDC. Also, the absorption bands at 1162, 3093, and 850 cm^{-1} are ascribed to C-N stretching, C-H aromatic, and C–H bending vibrations, respectively of the 2,6-pyridine dicarboxylic acid (PDC) ligand as a linker in the MOF configuration. The symmetric stretching vibration of Zn-O appearing around 540 - 749 cm^{-1} for all the samples, were also consistent with that of the literature [26].

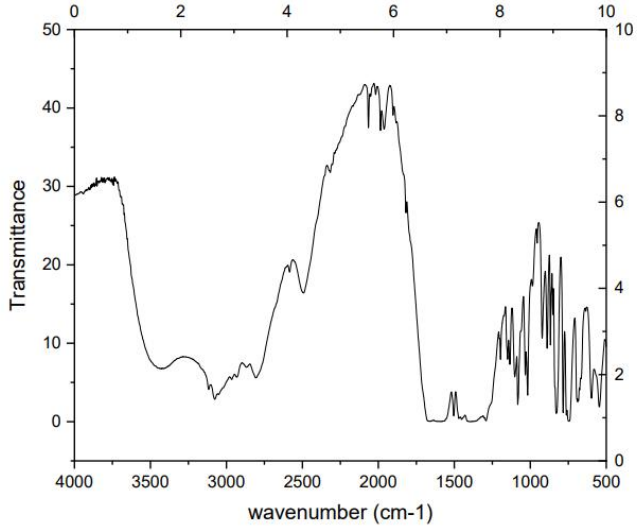

Figure 1. FTIR spectrum of MOF-5+PDC

X-ray Diffraction Analysis

Distinct and intense diffraction peaks were observed for the MOF-5 + PDC. The two strong peaks in the 2Θ region at 25° and 28.5°, corresponding to the pure MOF-5 diffraction pattern are associated with the 100 and 101 lattice planes, respectively, indicating that the MOF-5 crystalline compound has been successfully synthesized as seen in Figure 2 [27].

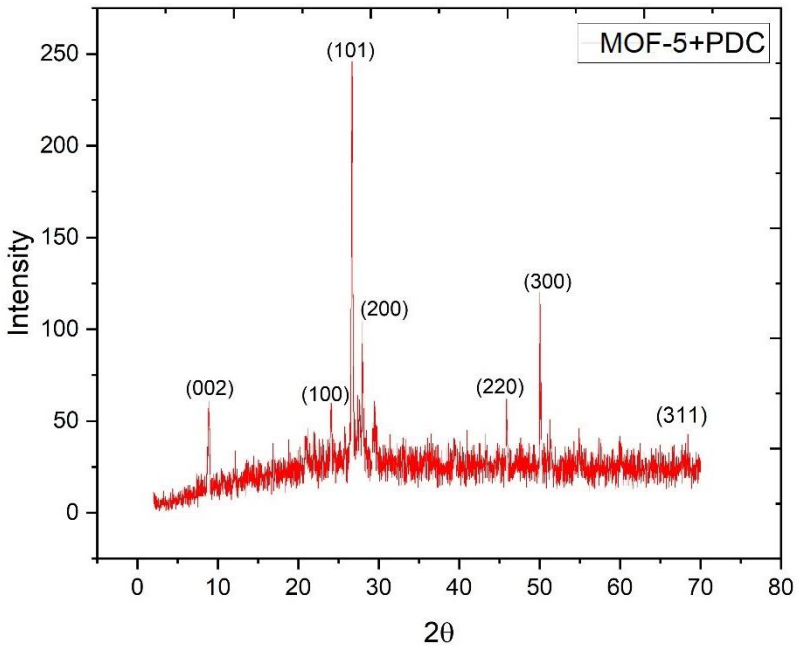

Figure. 2. X-ray diffraction spectra of MOF-5+PDC

A broad diffraction peaks that lies between 21.5° and 28.5° values of 2θ indicates pristine carbon (101), with little diffraction at 29.5° indicating (200). For PDC, the peaks at 2θ = 46.5°and 51.5° can be assigned (220) and (311) crystal planes, respectively [28].

SEM Analysis

The SEM micrographs of samples of MOF-5+PDC shows trapezoidal and porous surfaces which revealed irregular, rough, coarse surfaces with different cracks and crevices which reveal the existence of well-developed pores which is in agreement with [29] report. It is suggested that these pores could have resulted from the chemical activation.

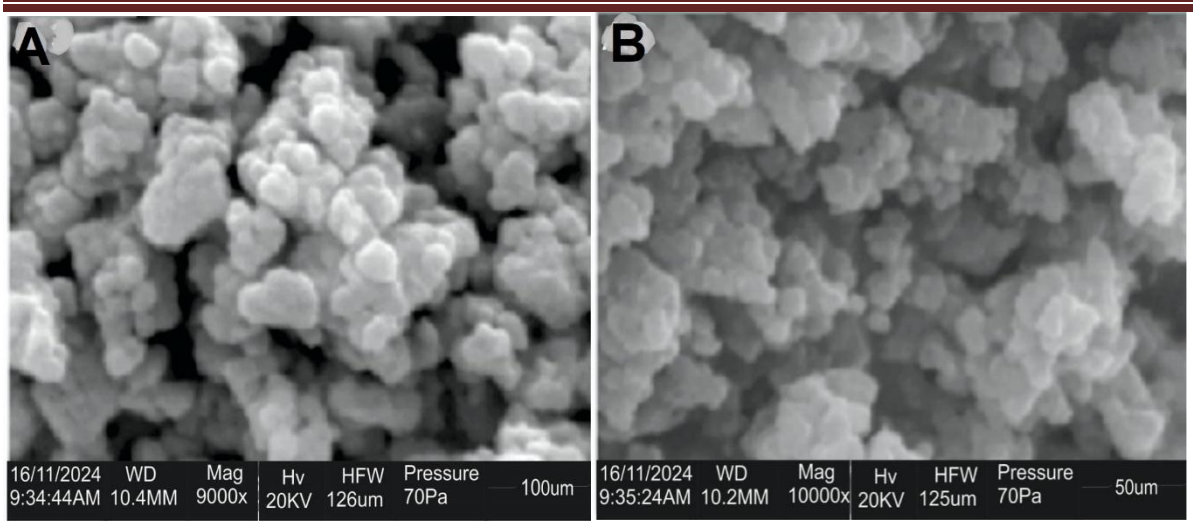

Figure 3. SEM Photograph of MOF-5+PDC a). 9000x and b). 10000x magnification

The developed pores could serve as the site for swallowing and trapping molecules when applied for adsorption and remediation. More so, the pores could also enhance the uninterrupted flow of adsorbate. The degree of devolatilization is an effective and important feature to achieve materials with specific density, higher porosity and unique pore structure [30].

N_2 Adsorption/Desorption Isotherm and Pore Size Analysis

N_2 adsorption/desorption isotherm of the synthesized MOF-5+PDC reveals type I isotherm at 77 K with no hysteresis phenomenon as seen in Figure 4a. The calculated BET surface area is 85.98 m^2/g for MOF-5+PDC sample. In the low relative pressure region, the adsorption curve of all the samples increases sharply which indicates the presence of micropores. The adsorption curve reached a plateau after that indicating that most of the MOF porosity is attributed to the micropores [3]. The calculated surface area, pore diameter and volume of the micropores was 272.76 m^2/g, 2.760 nm and 0.242 cm^3/g respectively for MOF-5+PDC.

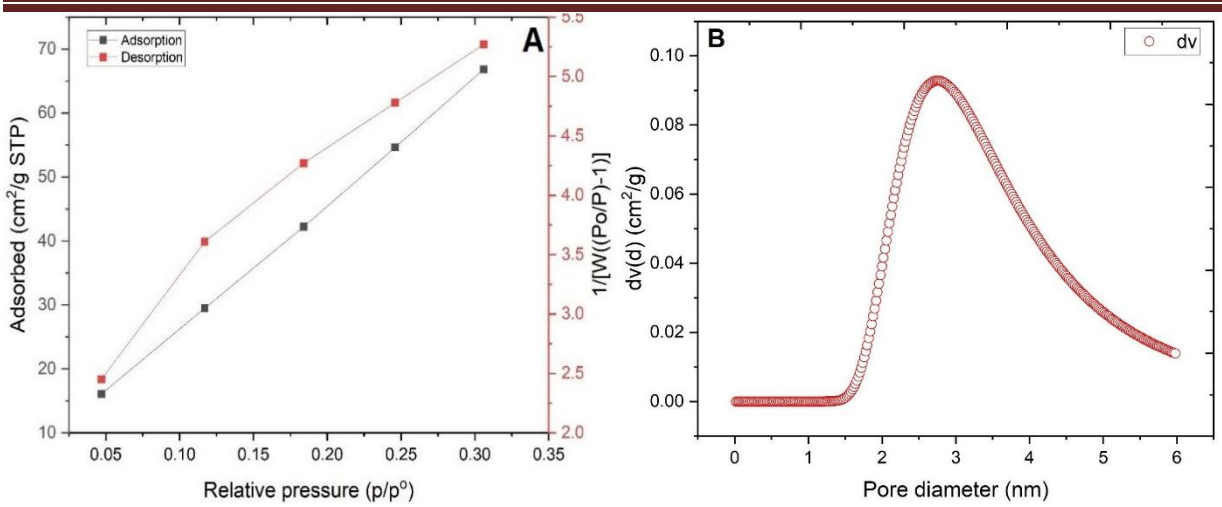

Figure 4. (a). N_2 adsorption/desorption isotherm of the sample and (b). Porosity size

The pore size distribution of the synthesized MOF-5+PDC reveals that the average pore diameter was 2.760 nm as seen in Figure (4b). More than 80% of the pores are micropores. The adsorption isotherms of N_2 on MOF-5+PDC reveal intriguing behavior, particularly its high adsorption capacity at low partial pressures. This phenomenon can be elucidated by considering the energy distribution of adsorption sites within the MOF structure [3]. The formation of porous material for MOFs could be explained by the formation of 2,6-pyridinedicarboxylic acid (PDC) and ZnO cluster in the sample structure, which could affect the reversible breathing behavior of these materials [31].

Thermo-gravimetric Analysis

The thermal stability of the MOF sample was studied by TGA and DTA. The sample exhibited a degradation evidenced by the observation of a peak in TGA curves as shown in Figure 5. There is no evidence of mass-loss up to 350°C, in good agreement with Yang et al [32]. Which occurs between 350°Cand 550°C with the total mass loss of 82% is attributed to the decomposition of MOF organic carboxylates [33].

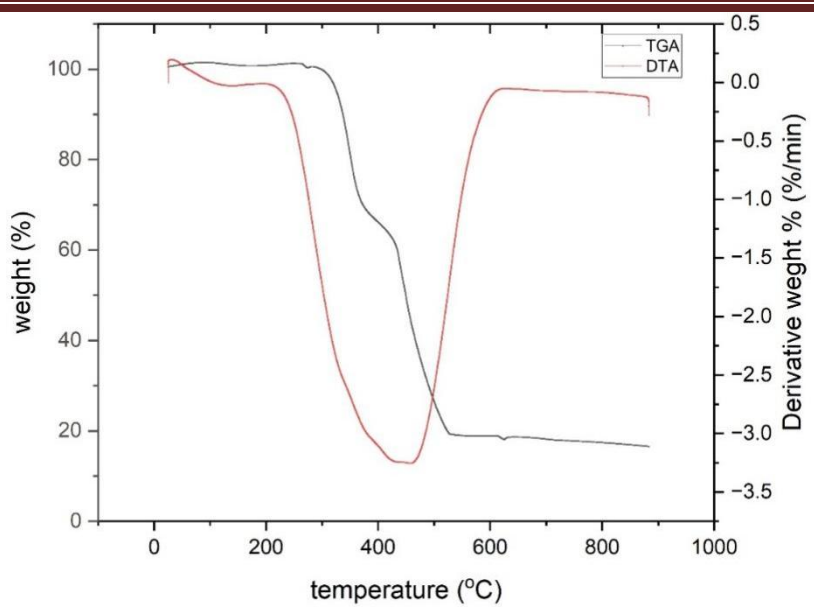

Figure 5: TGA and DTA curves of MOF-5+PDC

A little degradation occurred between 387 and 450˚C, the total mass loss was about 9%, reflecting the removal of solvent molecules and bound water molecules from within the pores of MOF sample. This amount of non-volatile molecules is inside MOF sample during the period of crystallization and washing. The DTA curve for MOF sample shows a clear peak at 475 °C indicating its decomposition and the gradual transition to ZnO [34].

FT-IR Analysis of MOF-5+PDC

The FT-IR spectral of sulfonic acid, cyano and amine functionalized-MOF-5+PDC displayed characteristic bands between 3435 and 3431 and cm^{-1} corresponded to O-H stretching**.** For SO_3H@MOF-5+PDC sample as presented in Figure 6, displayed the S=O functionality of sulfonic group stretching peaks are likely to be decomposed into several components, having asymmetric vibration components displaying peaks at 1203 cm^{-1}, while the symmetric stretching vibration appears at 994 cm-^{1} [35]. Figure 7 shows the FT-IR spectrum of cyano functionality CN@MOF-5+PDC displayed characteristic bands at 3431 cm^{-1} (corresponded to O-H stretching), 2288 cm^{-1} (assigned to C≡N stretching) of the cyano functionality.

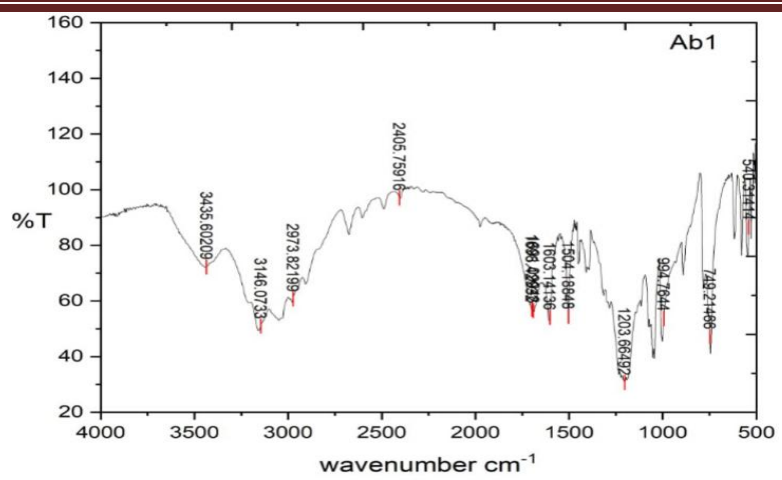

Figure 6: The FTIR spectrum of sulfonic functionality of SO_3H@MOF-5+PDC

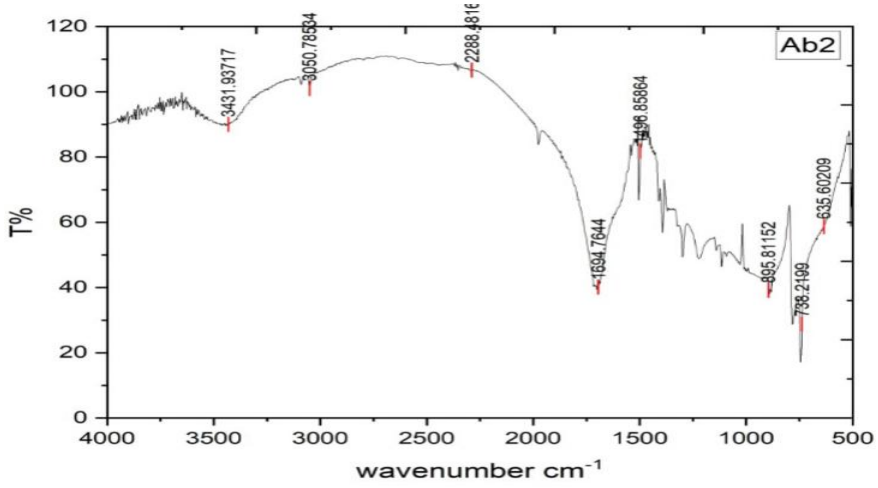

Figure 7: The FTIR spectrum of cyano functionality CN@MOF-5+PDC

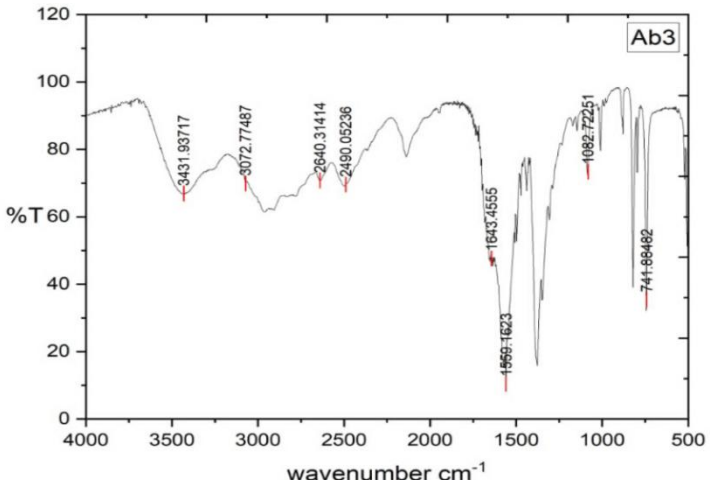

Figure 8: FTIR spectrum of amine functionality of NH_2@MOF-5+PDC

While Figure 8 shows the amine functionality of NH_2@MOF-5+PDC, a characteristic medium and weak stretching bands at 3072 – 2640 cm^{-1} and 3432-3072 cm^{-1} corresponded to the N-H group for both primary and secondary amine respectively were observed [36]. Also, absorption bands at. 1082 cm^{-1}, is correspond to C-N stretching vibrations of the amine group. The symmetric stretching vibration of Zn-O appearing around 540 - 749 cm^{-1} for all the samples.

Adsorption Experiments

The initial concentration of Pb(II) ion varied from 0.085±0.0021 - 0.1145±0.0021 ppm as depicted in Table 1. CN@MOF-5+PDC has the highest concentration of Pb (II) ion among the study MOFs. It was observed that the adsorption capacity (q) of the study MOFs was influenced by the concentration of Pb(II) metal ion. An increase in the initial concentration increased the quantity adsorbed by the MOFs. The adsorption capacity of the MOF adsorbent increased from 42/5 – 57.25 mg/g for Pb(II), as presented in Table 2 and Figures 9. CN@MOF-5+PDC has the highest adsorption capacity qe of 57.25, followed by NH_2@MOF-5+PDC with adsorption value of 49 and SO_3H@MOF-5+PDC has the least adsorption capacity of 42.5 mg/g.

Table 1. The initial metal ion concentration and adsorption capacity of the MOF adsorbents

MOF samples	Initial Concentration (ppm)	Adsorption capacity q(mg/g)
NH_2@MOF-5+PDC	0.098±0.0030	49
SO_3H@MOF-5+PDC	0.085±0.0028	42.5
CN@MOF-5+PDC	0.1145±0.0021	57.25

NH_2 = amine and PDC= pyridine-di-carboxylic acid

The adsorption capacity of CN@MOF-5+PDC adsorbents could be as a result of the pore size or increase in the electrostatic interaction between the metals and the absorbent active sites. Moreover, this can be explained by the fact that more adsorption sites were being covered as the metal ions concentration increases [37]. This indicated that the study MOFs structure had no destruction during the adsorption process. The adsorption behaviour for Pb(II) metal ions was excellent, where the removal efficiency was over 80 - 90.9% when the initial concentration of Pb(II) ions was as low as 0.066 ppm. Zhang et al [4] reported the successful adsorption removal of Pb(II) ions from aqueous samples by using a functionalized MOF-5. According to their report, functionalized- MOF-5 was shown to be a more convenient and effective adsorbent for Pb(II) ions than the pure MOF-5.

Thermodynamics Study

The data derived from the effect of temperature study were further used for the feasibility of the adsorption process of functionalized MOFs on Pb(II) metal ion. The results obtained from the thermodynamics study are shown in Tables 2.

Table 2. The thermodynamics analysis of the adsorption of Pb (II) metal ion

MOF samples	ΔH	ΔS	ΔG KJ/Mol		
	KJ/Mol	KJ/Mol	308K	318K	328K
NH_2@MOF-5+PDC	50433.937	164.538	-243.772	-1889.152	-3534.532
SO_3H@MOF-5+PDC	47105.762	152.374	174.465	-1349.278	-2873.021
CN@MOF-5+PDC	131813.326	421.820	1892.478	-2325.731	-6543.940

The enthalpy ΔH of all the study MOFs were positive, the positive value of heat of adsorption (ΔH) signifies an endothermic reaction for all the study MOFs. which indicated a favorable adsorption process for all the study MOFs. Only CN@MOF-5+PDC adsorbent has the lowest value of ΔH, which suggests that the adsorption process is likely to be physiosorption [39]. All the study MOFs have a positive value of ΔS. The positive value of entropy shows the increased degree of disorder of the adsorption system, which is caused by the range of Pb (II) ion movement being attracted by the adsorbent solid surface after the adsorption [40].

The positive values of entropy ΔS are an indication of an increased disorderliness and randomness at the adsorbent-sorbate interface and affinity for adsorbent material [41]. The Gibb's free energy values indicated that the degree of spontaneity of the sorption process. At 318 and 328K, the ΔG value of MOF adsorbents were negative, confirming the thermodynamic feasibility of adsorption of Pb(II) on the MOFs framework [42]. While at 308K, the ΔG value of the study MOF adsorbents for Pb(II) adsorption were positive except NH_2@MOF-5+PDC. Indicating non-spontaneous process at this temperature. Hence, need to improve the adsorbing capacity, at low temperature.

Optimization

The adsorption optimization of the study MOFs was carried out using the Box-Behnken Design module in response surface methodology to discover the best adsorption process of Pb(II) ions. The empirical model was created utilizing three optimization parameters as independent variables (concentration, pH, and dosage) production as the response (dependent variable) [43]. From the experimental data, it is inferred that the amount adsorbed in all seventeen experiments for all the studied MOFs at different conditions were within the range of 77.02 – 99.42 mg/g for Pb(II) adsorption.SO_3H@MOF-5+PDC has the highest adsorption of 99.42 mg/g, which was achieved at a concentration of 100 mg/L, pH of 7 and a dosage of 0.01 g, correlating to experimental run 16, standard 6, while the maximum amount adsorbed NH_2@MOF-5+PDC was 98.88 mg/g which was achieved at a concentration of 100 mg/L, pH of 10 and a dosage of 0.03 g, correlating to experimental run 13, standard 4, and for CN@MOF-5+PDC the maximum amount of Pb(II) ion adsorbed was 77.02 mg/g which was achieved at a concentration of 100 mg/L, at pH 7 and a dosage of 0.01 g, correlating to experimental run 16, standard 6.

Figures 9-11 show the predicted vs. actual plot adsorption of all the study MOFs for Pb(II) ion, There is a close distribution of data points between the actual experimental and predicted amount adsorbed along the straight line of the plot, demonstrating an excellent correlation between these values and confirming that the model adequately predicts the response variable in actual values.

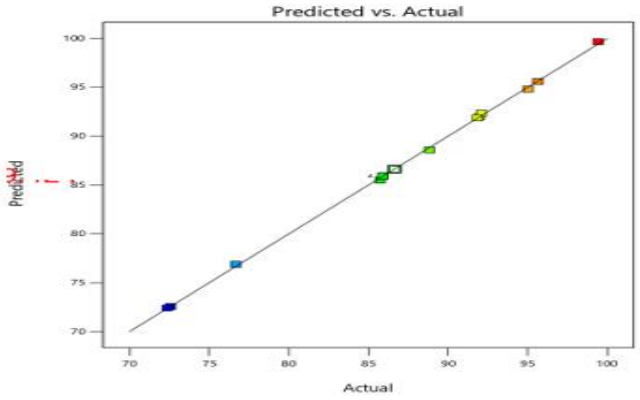

Figure 9: Graph showing predicted versus actual value for SO_3H-MOF-5@PDC for Pb(II) adsorption

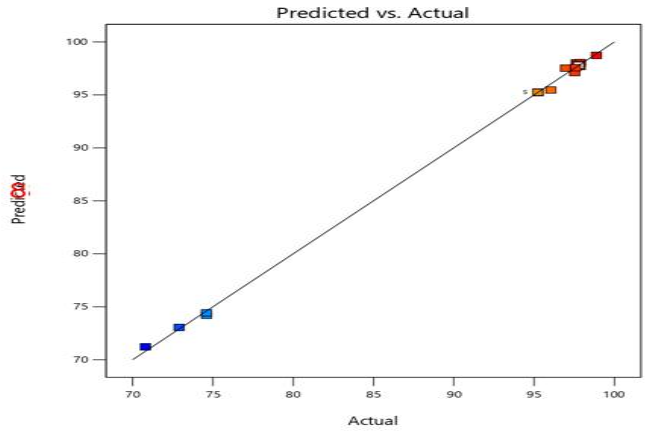

Figure 10: Graph showing predicted versus actual value for NH_2-MOF-5@PDC for Pb (II) adsorption

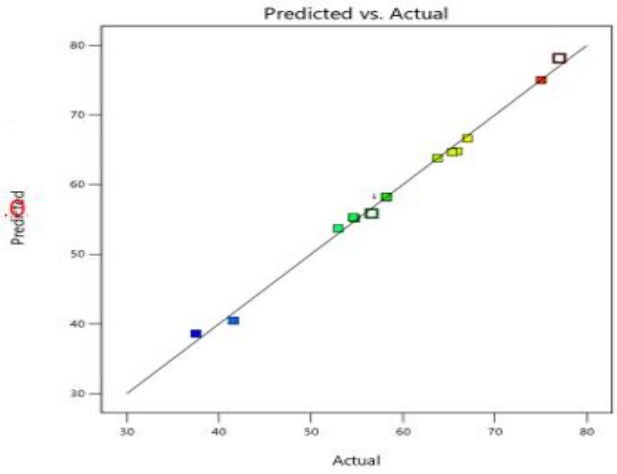

Figure 11: Graph showing predicted versus actual value for CN-MOF-5@PDC for Pb (II) adsorption

The ANOVA Quadratic model of MOFs for Adsorption of Pb(II) ions

The reaction conditions (concentration, pH and dosage) for the synthesis of amine functionalized MOFs were conducted using RSM (BBD) for experimental design. This is because these conditions affect the amount of Pb(II) ion adsorbed by the studied functionalized-MOFs. The model F-values of Pb(II) adsorption are 2124.86**,** 931.51 and177.50 for SO_3H@MOF-5+PDC**,** NH_2@MOF-5+PDC andCN@MOF-5+PDC respectively. All the model F-values of the studied

MOFs implied that the models are significant. Also, the p-values were less than 0.0500, indicating that the model terms are significant. In this case A, B, C, AB, AC, BC, A^2, B^2, C^2 are significant model terms. Values greater than 0.1000 indicate that the model terms are not significant. Where A, B, and C stand for concentration, pH, and dosage, respectively. The direct linear impacts of the independent process variables are represented by the coefficients A, B, and C. As opposed to AB, AC, and BC, which represent the linear interaction effects between molar ratio/temperature, molar ratio/time, and temperature/time, respectively, and A^2, B^2 and C^2 which depict the quadratic impacts of the independent process variables.

The Combined Effect Variables on Pb(II) Ions Adsorption

Effect of Concentration and pH (AB) on Adsorption

The 3D response surface plots for this combined effect were described in Figures 12a – c. From the surface plots, it was deduced that high adsorption yield was achieved at a high concentration and above pH 6. Therefore, in this study, an optimum percentage of yields could only be achieved at a high concentration and a pH above 6. Therefore, these results confirm the ANOVA results, which show that the combined effect of AB of all the study MOFs were significant with a p-value less than 0.005, except NH_2@MOF-5+PDC (0.6334) .

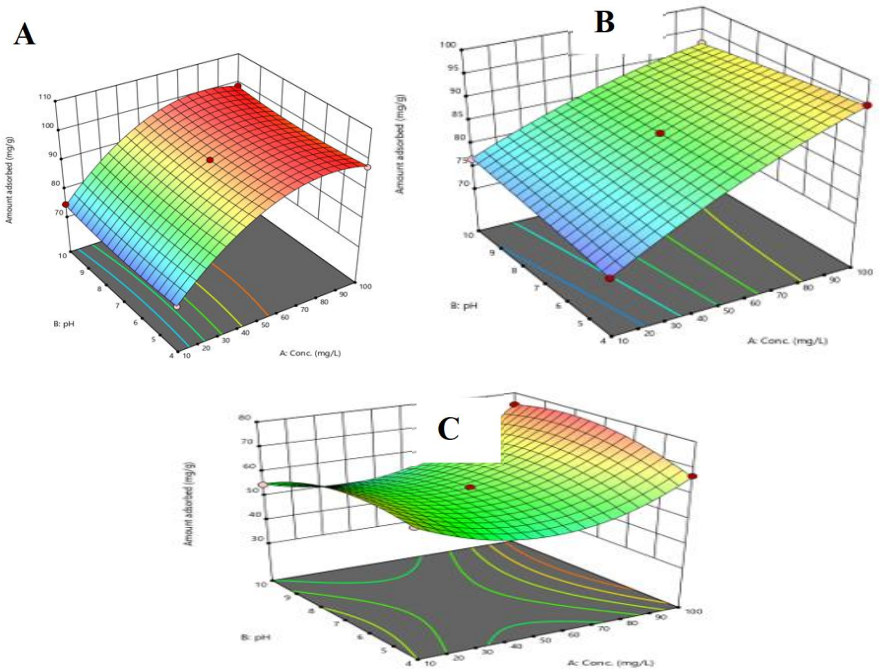

Figure 12**:** (a) Graph between concentration and pH a). NH_2@MOF-5+PDC, b). SO_3H@MOF-5+PDC and c). CN@MOF-5+PDC for Pb (II) adsorption.

Effect of Concentration and Dosage (AC) on Percentage Yield

Figure 13 reveals the 3D response surface plots. A high adsorption yield could be obtained at a high concentration and low dosage of (0.03 g). In this study, an optimum percentage of adsorption could be achieved at high concentration and low dosage. The ANOVA result shows that the combined effects of AC were significant with a p-value less than (< 0.0001) for all the studied MOFs, except NH_2@MOF-5+PDC which is 0.6864.

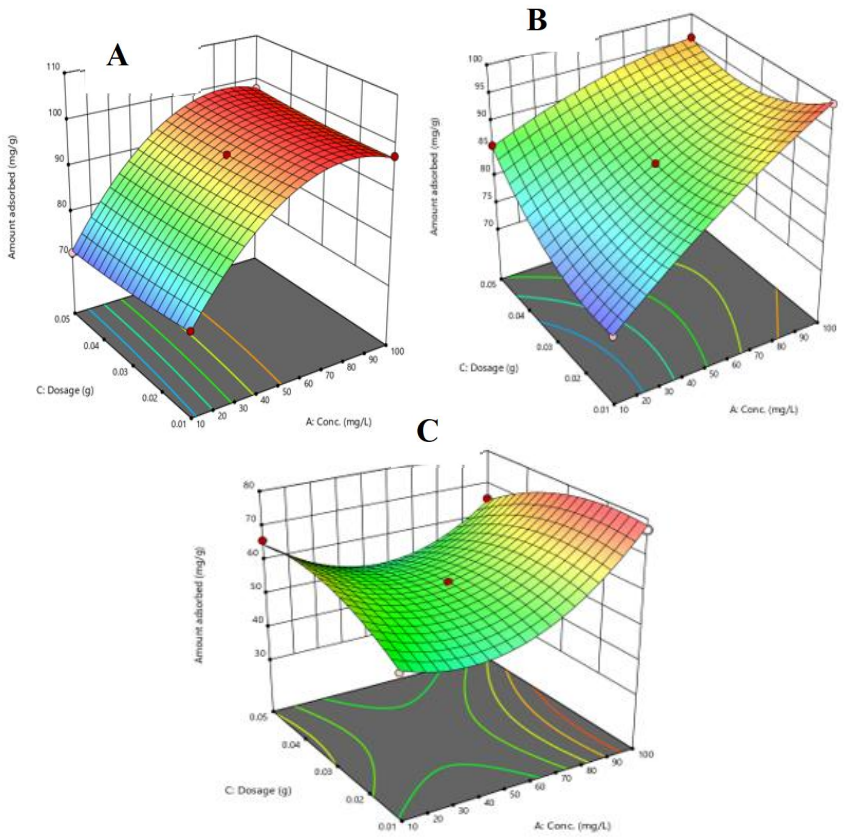

Figure 13: Graph between concentration and dosage a). NH_2@MOF-5+PDC, b). SO_3H@MOF-5+PDC and c). CN@MOF-5+PDC for Pb (II) adsorption

Effect of pH and Dosage

Figures 14 depicts the 3D for this effect that the highest adsorption yield was obtained at a low temperature and either a low or high reaction time. Lower adsorptions were observed at low pH and low dosage. This agreed with the conclusion from the ANOVA result, which indicates that the interaction effect of BC was significant for all the studied MOFs, with p-value less than 0.005.

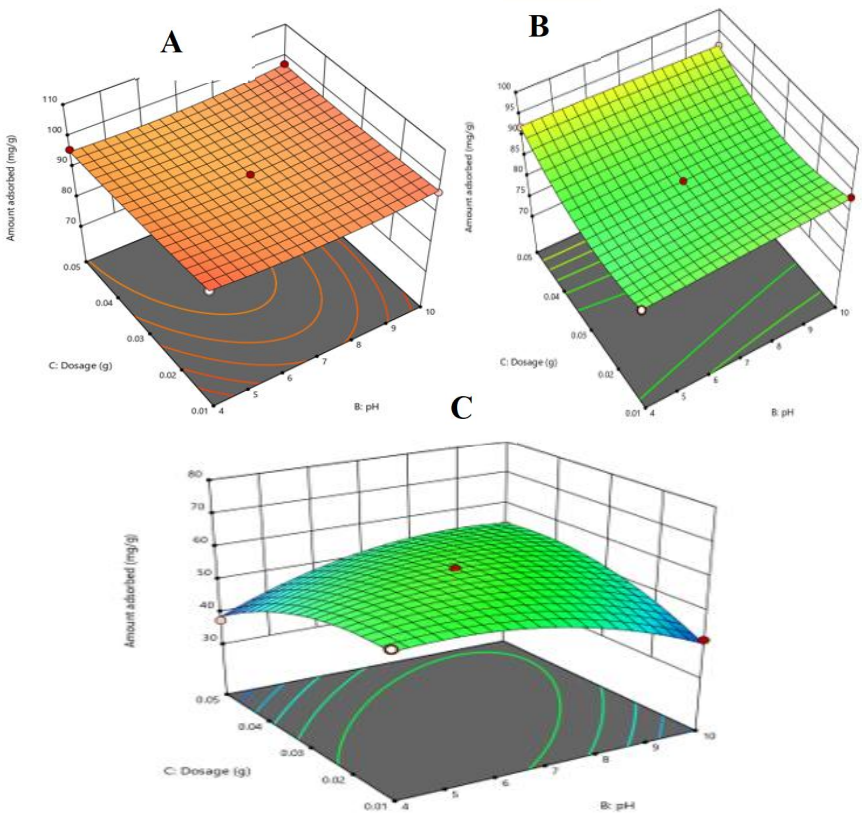

Figure 14**:** Graph between dosage and pH a). NH_2@MOF-5+PDC, b). SO_3H@MOF-5+PDC and c). CN@MOF-5+PDC for Pb (II) adsorption

CONCLUSION

In the present study, amine, cyano and sulfonic acid-functionalized MOF-5+PDC were synthesized by solvothermal and characterized by XRD, FTIR, SEM and EDX-mapping analysis to confirm the synthesis of MOF structures. The results of N_2 adsorption/desorption isotherm data showed that the BET surface area of the synthesized MOF-5+PDC sample was 85.98 m^2/g. The adsorption behaviour for Pb(II) metal ions revealed a very good adsorption capacity of 42.5 – 57.25 mg/g, whereas the removal efficiency was over 80 - 90.9% when the initial concentration of Pb(II) ions was as low as 0.066 ppm. Design of experiment for Pb(II) adsorption under optimal conditions of concentration, pH and dosage were within the range of 77.02 – 99.64 mg/g. In addition, thermodynamic analysis revealed that Pb(II) ion adsorption is a spontaneous

endothermic process. Based on the data from the study, these amine-functionalized MOFs are a promising adsorbent for the removal of Pb(II) ion from contaminated water.

REFERENCES

1. Wen, J., Fang, Y., & Zeng, G. (2018). Progress and prospect of adsorptive removal of heavy metal ions from aqueous solution using metal–organic frameworks: A review of studies from the last decade. *Chemosphere*, 201, 627-643. https://doi.org/10.1016/j.chemosphere.2018.03.047
2. Kumar, A., Kumar, A., Cabral-Pinto, M.M.S., Chaturvedi, A.K., Shabnam, A.A., Subrahmanyam, G., Mondal, R., Gupta, D.K., Malyan, S.K., Kumar, S.S., Khan, S.A., & Yadav, K.K. (2024). Introduction of heavy metals contamination in the water and soil: a review on source, toxicity and remediation methods. *Green Chemistry Letters and Reviews*, 17(1), 2404235. https://doi.org/10.1080/17518253.2024.2404235
3. Waheed, A., Umair, B., Lukka, T. Y., & Isma, A. (2024). Tailored alumina nanocomposite organic frameworks for oily wastewater treatment, npj *Clean Water* 7(1), 1–12. https://doi.org/10.1038/s41545-024-00321-w
4. Zhang, J., Xiong, Z., Li, C., & Wu, C. (2016). Exploring a thiol-functionalized MOF for elimination of lead and cadmium from aqueous solution. *Journal of Molecular Liquids*, *221*, 43–50. https://doi.org/10.1016/j.molliq.2016.05.054
5. Khajeh, M., Heidari, Z. S., &Sanchool, E. (2011). Synthesis, characterization, and removal of lead from water samples using lead-ion imprinted polymer. *Chemical Engineering Journal*, *166*, 1158–1163.
6. Lingamdinne, L. P., Chang, Y. Y., Yang, J. K., Singh, J., Choi, E. H., Shiratani, M., &Attri, P. (2017). Biogenic reductive preparation of magnetic inverse spinel iron oxide nanoparticles for the adsorption removal of heavy metals. *Chemical Engineering Journal*, *307*, 74–84. https://doi.org/10.1016/j.cej.2016.08.067
7. Wang, C., He, C., Luo, Y.-H., Su, S., Wang, J.-Y., Hong, D.-L., He, X.-T., Chen, C., & Sun, B.-W. (2020). Efficient mercury chloride capture by ultrathin 2D metal–organic framework nanosheets. *Chemical Engineering Journal*, *379*, 122337.

8. Fang, Q. R., Yuan, D. Q., Sculley, J., Li, J. R., Han, Z. B., & Zhou, H. C. (2010). Functional mesoporous metal–organic frameworks for the capture of heavy metal ions and size-selective catalysis. *Inorganic Chemistry*, *49*, 11637–11642.
9. Lucena, M. A., Oliveira, M. F., Arouca, A. M., Talhavini, M., Ferreira, E. A., Alves Jr, S., Veiga-Souza, F. H., & Weber, I. T. (2017). Application of the metal–organic framework [Eu(BTC)] as a luminescent marker for gunshot residues: A synthesis, characterization, and toxicity study. *ACS Applied Materials & Interfaces*, *9*, 4684–4691.
10. Mi, X., Sheng, D., Yu, Y., Wang, Y., Zhao, L., Lu, J., Li, Y., Li, D., Dou, J., Duan, J., & Wang, S. (2019). Tunable light emission and multiresponsive luminescent sensitivities in aqueous solutions of two series of lanthanide metal–organic frameworks based on structurally related ligands. *ACS Applied Materials & Interfaces*, *11*, 7914–7926.
11. Efome, J. E., Rana, D., Matsuura, T., & Lan, C. Q. (2018). Metal–organic frameworks supported on nanofibers to remove heavy metals. *Journal of Materials Chemistry A*, *6*, 4550–4555.
12. Tesh, S. J., & Scott, T. B. (2014). Nanocomposites for water remediation: A review. *Advanced Materials*, *26*, 6056–6068.
13. Hwang, Y. K., Hong, D. Y., Chang, J. S., Jhung, S. H., Seo, Y. K., Kim, J., Vimont, A., Daturi, M., Serre, C., &Férey, G. (2008). Amine grafting on coordinatively unsaturated metal centers of MOFs: Consequences for catalysis and metal encapsulation. *AngewandteChemie International Edition*, *47*, 4144–4148.
14. Wu, C. D., & Zhao, M. (2017). Incorporation of molecular catalysts in metal–organic frameworks for highly efficient heterogeneous catalysis. *Advanced Materials*, *29*, 1605446.
15. Feng, M., Zhang, P., Zhou, H.-C., & Sharma, V. K. (2018). Water-stable metal–organic frameworks for aqueous removal of heavy metals and radionuclides: A review. *Chemosphere*, *209*, 783–800.
16. Ming, Y., Kumar, N., & Siegel, D. J. (2017). Water adsorption and insertion in MOF-5. *ACS Omega,* 2, 4921–4928.

17. Wibowo, A., Marsudi, M. A., Pramono, E., Belva, J., Parmita, A. W. Y. P., Patah, A., Eddy, D. R., Aimon, A. H., & Ramelan, A. (2021). Recent improvement strategies on metal–organic frameworks as adsorbent, catalyst, and membrane for wastewater treatment. *Molecules*, *26*, 5261. https://doi.org/10.3390/molecules26175261

18. Cai, X. Q., Li, J. H., Zhang, Z., Yang, F. F., Dong, R. C., & Chen, L. X. (2014). Novel Pb^{2+} ion imprinted polymers based on ionic interaction via synergy of dual functional monomers for selective solid-phase extraction of Pb^{2+} in water samples. *ACS Applied Materials & Interfaces,* 6, 305–313.

19. Goel, J., Kadirvelu, K., Rajagopal, C., & Garg, V. K. (2005). Removal of lead(II) by adsorption using treated granular activated carbon: Batch and column studies. *Journal of Hazardous Materials,* 125(1-3), 211-220.

20. Sari, A., Tuzen, M., Citak, D., &Soylak, M. (2007). Equilibrium, kinetic and thermodynamic studies of adsorption of Pb(II) from aqueous solution onto Turkish kaolinite clay. Journal of Hazardous Materials, 149, 283–291.

21. Adly, M. S., El-Dafrawy, S. M., Ibrahim, A. A., El-Hakam, S. A., & El-Shall, M. S. (2021). Efficient removal of heavy metals from polluted water with high selectivity for Hg(II) and Pb(II) by a 2-imino-4-thiobiuret chemically modified MIL-125 metal–organic framework. *RSC Advances,* 11, 13940.

22. Li, C., Wang, J., Wan, J., & Yu, C. (2021). MOF-on-MOF hybrids: Synthesis and applications. *Coordination Chemistry Reviews,* 432, 213743.

23. Luo, X., Ding, L., & Luo, J. (2015). Adsorptive removal of Pb(II) ions from aqueous samples with amino-functionalization of metal–organic frameworks MIL-101(Cr). *Journal of Chemical & Engineering Data,* 60(2), 101–110. https://doi.org/10.1021/je501115m

24. Guo, J., Wang, Y., Lan, Z., Huang, X., & Liu, H. (2019). Study on catalytic effect and mechanism of MOF (MOF = ZIF-8, ZIF-67, MOF-74) on hydrogen storage properties of magnesium. *International Journal of Hydrogen Energy*, 44(54), 28863–28873.

25. Jimoh, A. A., Adebayo, G. B., Otun, K. O., Ajiboye, A. T., & Bale, A. T. (2015). Sorption study of Cd(II) from aqueous solution using activated carbon prepared from Vitellaria paradoxa shell. *Journal of Bioremediation & Biodegradation*, 6, 288. https://doi.org/10.4172/2155-6199.1000288
26. Ahmad, S., Badshah, A., Muhammad, H., Jawad, M., Mustansar, S., Ali, U., & Khan, S. U. (2018). Synthesis of highly stable MOF-5 @ MWCNTs nanocomposite with improved hydrophobic properties. *Arabian Journal of Chemistry,* 11(1), 26–33. https://doi.org/10.1016/j.arabjc.2017.01.012.
27. Aghajani, M. J., Ghani, M., & Raoof, J. B. (2024). Synthesis of MOF-5 modified Bi_2WO_6 polyoxometalate accommodated on the pores of hollow fiber for HF-SPME of acetamiprid, abamectin and diazinon and their determination by high-performance liquid chromatography–ultraviolet. *Microchemical Journal*, 8, 279–292.
28. Zhang, J., & Ma, Z. (2017) Flower-like Ag 3 VO 4 /BiOBr n-p heterojunction photocatalysts with enhanced visible-light-driven catalytic activity. *Mol Catal* 436:190–198. https://doi.org/10.1016/j.mcat.2017.04.004.
29. Kim, H., Das, S., Kim, M. G., Dybtsev, D. N., Kim, Y., & Kim, K. (2011). Synthesis of phase-pure interpenetrated MOF-5 and its gas sorption properties. *Inorganic Chemistry*, 50, 3691–3696.
30. Chaikittisilp, W.; Suzuki, Y.; Mukti, R. R.; Suzuki, T.; Sugita, K.; Itabashi, K.; Shimojima, A.; Okubo, T. (2013) Formation of Hierarchically Organized Zeolites by Sequential Intergrowth. *Angew. Chem., Int. Ed*., 52, 3355−3359
31. Vuong, G.-T.; Pham, M.-H.; Do, T.-O. (2013). Direct synthesis and mechanism of the formation of mixed metal Fe2Ni-MIL-88B. *CrystEngComm,* 15, 9694.
32. Yang, S. J., Kim, T., Im, J. H., Kim, Y. S., Lee, K., Jung, H., & Park, C. R. (2012). MOF-derived hierarchically porous carbon with exceptional porosity and hydrogen storage capacity. *Chemistry of Materials,* 24(3), 464–470.
33. Zhang, R., Wilson, V.L., Hou, A., & Meng, G. (2015). Source of lead pollution, its influence on public health and the countermeasures. International Journal of Health, *Animal Science and Food Safety,* 2(1).

34. Mayedwa, N., Khalil, A.T., Mongwaketsi, N., Matinise, N., Shinwari, Z.K. & Maaza, M. (2017). The study of structural, physical and electrochemical activity of ZnO nanoparticles synthesized by green natural extracts of *sageretia thea, Nano Res. Appl*. 3 (2017) 1–9.
35. Nivetha, R., Kollu, P., Chandar, K., Pitchaimuthu, S., Jeong, S. K., & Grace, A. N. (2019). RSC Advances Role of MIL-53 (Fe)/ hydrated – dehydrated MOF catalyst for electrochemical hydrogen evolution reaction (HER) in alkaline medium and. *RSC Advances,* 9, 3215–3223. https://doi.org/10.1039/C8RA08208A
36. Hu, S., Liu, M., Li, K., Zuo, Y., Zhang, A., Song, C., Zhang, G., & Guo, X. (2014). Solvothermal synthesis of NH2-MIL-125(Ti) from circular plate to octahedron. *CrystEngComm*, 16(January 2017), 9645–9650. https://doi.org/10.1039/C4CE01545B
37. Mohan, D., & Singh, K. P. (2002). Single and multi-component adsorption of cadmium and zinc using activated carbon derived from bagasse—an agricultural waste. *Water Research,* 36, 2304–2318.
38. Hema, M., & Arivoli, S. (2007). Comparative study on the adsorption kinetics and thermodynamics of dyes onto acid activated low-cost carbon. *International Journal of Physical Sciences,* 2, 10–17.
39. Xiang, G. G., Sen Q., Xiuting, C., Yu G., and Xiaoqi S., (2017) Postsynthesis Modification of a Metallosalen-Containing Metal−Organic Framework for Selective Th(IV)/Ln(III) Separation. *Inorg. Chem.* 56, 12357−1236. DOI: 10.1021/acs.inorgchem.7b01835
40. Lawal, O. S., Sanni, A. R., Ajayi, I. A., & Rabiu, O. O. (2010). Equilibrium, thermodynamic and kinetic studies for the biosorption of aqueous lead(II) ions onto the seed husk of Calophylluminophyllum. *Journal of Hazardous Materials*, 177, 829–835.
41. Chowdhury, S., Mishra, R., Saha, P., & Kushwaha, P. (2011). Adsorption thermodynamics, kinetics and isosteric heat of adsorption of malachite green onto chemically modified rice husk. *Desalination*, 265, 159–168.
42. Jumaah, A., Salih, N., & Salimon, J. (2022). D-optimal design optimization for esterification of palm fatty acids distillate with polyhydric alcohols for biolubricants production. *Iranian Journal of Chemistry and Chemical Engineering*, 41(5), 1657–1672.